European Journal of Agronomy 144 (2023) 126757

Contents lists available at ScienceDirect

European Journal of Agronomy

journal homepage: www.elsevier.com/locate/eja

# A robust field-based method to screen heat tolerance in wheat

Najeeb Ullah [a,b,*], Jack Christopher [a], Troy Frederiks [c], Shangyu Ma [a,d], Daniel KY Tan [e], Karine Chenu [a,**]

[a] The University of Queensland, Queensland Alliance for Agriculture and Food Innovation (QAAFI), Leslie Research Facility, 13 Holberton Street, Toowoomba, QLD 4350, Australia
[b] Agricultural Research Station, Office of VP for Research & Graduate Studies, Qatar University, 2713, Doha, Qatar
[c] Department of Agriculture and Fisheries, 203 Tor Street, Toowoomba, QLD 4350, Australia
[d] School of Agronomy, Anhui Agricultural University, Hefei, Anhui, China
[e] The University of Sydney, Plant Breeding Institute, Sydney Institute of Agriculture, School of Life and Environmental Sciences, Faculty of Science, Sydney, NSW 2006, Australia

ARTICLE INFO

*Keywords:*
Phenotyping
Heat stress
Genotype x environment interaction
Crop improvement
Breeding
Photoperiod extension

ABSTRACT

Wheat is highly sensitive to heat shocks and their timing. Hence, field-based ranking for heat tolerance may be confounded by phenological variations at the time of heat events. A photoperiod-extension method (PEM) was developed, allowing screening of wheat genotypes at matched developmental stages despite phenological variations. Paired trials were conducted to compare PEM and conventional field screening. In the PEM, artificial lighting was installed at one end of each row, inducing a gradient of flowering times. Individual stems or plot quadrats of each genotype were tagged at flowering. Late-sown plants experienced significantly more heat and greater grain yield reductions than early sown plants. Strong correlations between trials experiencing a similar degree of heat were found both for individual grain weight (IGW) and total grain weight with the PEM, either with individual stem tagging or quadrat tagging. By contrast, correlations for IGW and yield in these environments were either poor or negative for conventional trials. With the PEM, strong genetic correlations were found between irrigated environments of similar heat stress, with respective r correlations ranged from 0.46 to 0.8 for IGW; and 0.54–0.75 for total grain weight. By contrast these correlations were substantially weaker for conventional yield plots (average r values ranged from 0.11 to 0.53 for IGW; and 0.05–0.36 for grain yield. The quadrat sampling appeared overall more suitable for high-throughput phenotyping. The method promises to improve the efficiency of heat tolerance field screening, particularly when comparing genotypes of different maturity types.

## 1. Introduction

Climate variability is among the major determinants of global crop yields, including wheat (Najeeb et al., 2019; Ray et al., 2015) and strongly impedes plant breeding (Chapman et al., 2012). A significant increase in the frequency of heat stress events, particularly during grain filling has been recorded in the major wheat production regions such as Australia during the past 30 years (Ababaei and Chenu, 2020). These heat events have substantially affected the growth, development and ultimately yield of wheat crops (e.g. Ababaei and Chenu, 2020; Zheng et al., 2016), and are impacting optimal management practices (e.g. Collins and Chenu, 2021; Lobell et al., 2015; Zheng et al., 2012). With the recent rate of climate change, a further increase in the frequency of these heat events is projected in the near future both in Australia (Collins and Chenu, 2021) and globally (Field et al., 2012). Thus, developing wheat genotypes with superior heat tolerance during grain filling is critical for sustaining wheat grain yields and maintaining food security in future hot climates (Ullah et al., 2020).

Wheat is highly sensitive to elevated temperatures, and the impact of heat stress is strongly dependent on the crop developmental stage (e.g. Chenu and Oudin, 2019; Fernie et al., 2022; Prasad and Djanaguiraman, 2014). Reproductive and grain filling phases of wheat are extremely sensitive to heat, and even a mild increase in the atmospheric temperature during these stages can significantly reduce grain yield. For

* Corresponding author at: Agricultural Research Station, Office of VP for Research & Graduate Studies, Qatar University, 2713, Doha, Qatar.
** Corresponding author.
*E-mail addresses:* n.ullah@uq.edu.au (N. Ullah), karine.chenu@uq.edu.au (K. Chenu).

https://doi.org/10.1016/j.eja.2023.126757
Received 11 June 2022; Received in revised form 5 November 2022; Accepted 30 December 2022
Available online 25 January 2023

example, a single hot day (>30 °C) during the early reproductive stage or the onset of meiosis in pollen or micro / megaspore development can completely sterilise the developing wheat pollen (Saini and Aspinall, 1982). The effect of high temperature on pollen typically translates into a poor grain set and grain yield loss (Guo et al., 2016). Each degree increase (from 15° to 22°C) in mean temperature during pollen developmental can reduce grain number per unit area by 4 %, while a degree increase in maximum temperature at mid anthesis can also result in a 4 % reduction in grain number in wheat (Wheeler et al., 1996).

Post-anthesis heat reduces grain yield primarily by limiting assimilate synthesis, translocation, and starch deposition to developing grains (Sofield et al., 1977). Grain weight is most sensitive to heat during early grain filling and becomes progressively less sensitive as grain filling proceeds (Stone and Nicolas, 1995). A single hot day (maximum temperature of 40 °C) occurring 10–13 days after anthesis can reduce individual grain weight (IGW) by 14 % (Stone and Nicolas, 1998). In addition, IGW loss may be reduced by 0.5 % for each day delay in exposure to heat stress between 15 and 35 days after anthesis (Stone and Nicolas, 1995). Reduction in IGW of heat stressed plants is strongly linked with a shortened grain filling duration (Stone and Nicolas, 1995; Girousse et al., 2021). It has been reported in wheat crops that for each °C rise in mean daily temperature above optimum (15–20 °C), there can be a two to eight day reduction in grain filling duration (reviewed by Streck, 2005). In the Australian wheatbelt, a steady increase in the frequency of hot days ($T_{max}$ > 26 °C) during the grain filling period of wheat crops has been recorded over the past 30 years (Ababaei and Chenu, 2020). These authors also pointed out that heat-induced yield losses due to reduced grain weight (18.1 %) were greater than those due to grain number (3.6 %). This highlights the importance of developing wheat germplasm more tolerant to heat post-flowering.

Conventionally, wheat genotypes are screened for heat tolerance by serial sowings, using heat chambers in the field, or in controlled environments (e.g. Telfer et al., 2021, 2018; Thistlethwaite et al., 2020). Ranking for heat tolerance is typically based on physiological or morphological traits associated with plant function and performance (Bennett et al., 2012). However, changes in these traits are strongly influenced by the environment and the methodology used (Limpens et al., 2012; Poorter et al., 2016). Field-based screening methods are generally considered more representative of the plant response to natural environments (Passioura, 2006). However, screening of wheat genotypes with varying maturity types may be complicated by the unpredictability of heat events under field conditions. The impact of heat events is highly dependent on the developmental phase (e.g. Chenu and Oudin, 2019; Djanaguiraman et al., 2014; Tashiro and Wardlaw, 1990), which is specific to each particular wheat line being tested. Thus, the ranking of wheat genotypes for heat tolerance may be confounded by variation in the developmental stage during a natural heat event. An improved technique to screen for high temperature stress at matched developmental stages of wheat genotypes in the field could accelerate the selection of heat tolerant genotypes.

The impact of light intensity and duration on the growth and development of crops has been extensively explored (reviewed by Poorter et al., 2019). For example, with the increasing incident light intensity, the phenology of wheat and barley crops could be accelerated both under short (10 h) and long (16 h) days (Paleg and Aspinall, 1964). Due to this regulatory control of daily integrated light (mol $m^{-2}$ $d^{-1}$) on the phenology of crops (Poorter et al., 2019), artificially supplemented light has been used for manipulating the timing of wheat flowering (Frederiks et al., 2012). The intensity of incident light changes as a function of distance from its source (Niinemets and Keenan, 2012) and thus could manipulate wheat phenology in such a way as to induce multiple flowering dates from a single sowing date.

Here, we developed and tested a photoperiod-extension method (PEM) that allows the comparison of the performance of wheat genotypes with varying maturity types at common developmental stages during natural heat events. The method was tested across three different locations over three consecutive years, harvesting either specific spikes that flowered at the same time or small areas of plants (i.e. quadrats) flowering the same day (i.e. 50 % of the spikes at anthesis). The ranking of wheat genotypes with varying maturity types and heat tolerance were compared using PEM and conventional plots.

## 2. Materials and methods

### 2.1. Growth conditions and experimental design

Field trials were conducted over three consecutive years (2018–2020) at three southern Queensland, Australia, locations. Heavy black cracking clay soils with high moisture holding capacity predominated at all sites. Soils were deep and able to store moisture over the growing season. Conventional plots were established adjacent to trials using the newly developed photoperiod-extension method (PEM). Randomised block design trials with two times of sowing blocks and four replicates were established each year. To maximise the likelihood of heat stress during grain filling, trials were planted typically later in the cropping season than industry practice (Table 1). At the University of Queensland Research Farm, Gatton (27°34′50″S, 152°19′28″E), the first sowings (tSow1) were established between late May or early July and the second sowings (tSow2) between late August or early September. At the Hermitage Research Station, Warwick (28°12’40’’S, 152°06’06’’E), trials were sown in early June or mid-July (tSow1) or mid-August and mid-September (tSow2). At the Tosari Crop Research Centre, Tummaville (27°49’09.1"S 151°26’14.9"E), plants were sown in mid-July (tSow1) and early September (tSow2). All trials were fully irrigated (except at Tosari) and cultivated under non-limiting fertiliser conditions (Table 1). A boom irrigator was used for irrigating plots at Gatton (2018–2020) as well as both plot and PEM trials at Tosari. PEM trials at Gatton (2018–2020) and Warwick (2018) were irrigated with wobbler sprinklers. In 2020, both PEM and conventional plots trials at Warwick were irrigated using a drip irrigation system. At Tosari, trials were irrigated at sowing and pre-flowering, but no post-flowering irrigation was applied due to restricted water availability. For all trials, standard crop management practices, including weed, disease and pest control, were adopted during the season.

With the PEM, each wheat genotype was either hand sown in a 5 m single row (33 cm row spacing) in 2018 and 2019 or machine planted in a four-row plot (1 × 5 m, 2020 with 25 cm row spacing).

Conventional field plots were planted on the same day and with similar management to the PEM trials. In 2018 and 2020, the conventional field plots (2 × 6 m) were set up in Gatton and Warwick, while in 2019, genotypes were tested in smaller plots (1 × 6 m) at Tosari and Gatton. All conventional plots were planted at a 25 cm row spacing with a population density of 130 plants $m^{-2}$ and in four independent replications. Due to the unavailability of irrigation water, only sowing 2 (tSow2) plots were established at Gatton during 2018.

Trials are given identifiers denoting the site (Gatton (GAT), Tosari (TOS) or Warwick (WAR), and the year of the trial. Data may also be identified by the time of sowing (tSow1 or tSow2) and the tagging event (T1, T2, T3) when applicable.

### 2.2. Genotypes

Thirty-five wheat (*Triticum aestivum* L.) genotypes with contrasting phenology and adaptation were used in the study (Table S1, Supplementary). These included high-performing spring cultivars Suntop, Spitfire, Gregory, Janz, Hartog, EGA Wylie, Corack, Yitpi, Mace and Scout widely cultivated in major cropping regions of Australia. A set of eight CIMMYT genotypes described as heat tolerant under Australian environments was obtained from the University of Sydney (Thistlethwaite et al., 2020). Other genotypes used in these trials included donors of a multi-reference parent nested association mapping (MR-NAM) population developed for screening for heat and drought

**Table 1**
Trial characteristics, including the trial identifier (Trial), site, irrigation treatment, sowing date and the types of the trial conducted (i.e. PEM with tagging and harvesting of either single spikes or quadrates; and conventional plots). Also presented are post-flowering mean and max daily temperature, day-time vapour pressure deficit (VPD) and radiation from sowing to maturity, as well as the mean duration of the pre- and post-flowering periods, and the heat environment type (HET) for the first tagging of trials with the photoperiod-extension method (PEM). Days to flowering and post-flowering duration were calculated from sowing to flowering and flowering to maturity, respectively. TOS19 trial only had supplementary pre-flowering irrigation and experienced mild post-flowering water stress.

| Trial | Site | Time of sowing | Trial type | Sowing date | Irrigation | Mean temp. (°C) | Mean daily max temp. (°C) | Mean VPD (kPa) | Mean daily radiation (MJ $m^{-2}$) | Days to flowering (days) | Post-flowering duration (days) | HET |
|---|---|---|---|---|---|---|---|---|---|---|---|---|
| GAT18-s1 * | Gatton | tSow1 | Spike & quadrate PEM | 03/07/2018 | Full | 19.3 | 26.3 | 0.74 | 23.8 | 73 | 42 | HET1 |
| GAT18-s2 | Gatton | tSow2 | Spike & quadrate PEM,& plots | 31/08/2018 | Full | 23.1 | 31.4 | 1.38 | 23.2 | 53 | 39 | HET2 |
| WAR18-s1 | Warwick | tSow1 | Spike & quadrate PEM | 16/07/2018 | Full | 18.6 | 25.6 | 0.84 | 17.7 | 73 | 39 | HET1 |
| WAR18-s2 | Warwick | tSow2 | Spike & quadrate PEM | 12/09/2018 | Full | 22.0 | 30.3 | 1.52 | 21.2 | 52 | 37 | HET2 |
| GAT19-s1 | Gatton | tSow1 | Spike PEM & plots | 09/07/2019 | Full | 19.5 | 28.7 | 1.40 | 16.8 | 71 | 39 | HET2 |
| GAT19-s2 | Gatton | tSow2 | Spike PEM & plots | 03/09/2019 | Full | 23.7 | 33.8 | 2.23 | 20.8 | 59 | 35 | HET3 |
| TOS19-s1 | Tosari | tSow1 | Spike & quadrate PEM, & plots | 16/07/2019 | Supplementary | 21.1 | 30.2 | 1.26 | 17.7 | 79 | 35 | HET2 |
| TOS19-s2 | Tosari | tSow2 | Spike PEM & plots | 06/09/2019 | Supplementary | 26.5 | 36.7 | 2.27 | 22.2 | 62 | 35 | HET3 |
| GAT20-s1 | Gatton | tSow1 | Quadrate PEM & plots | 26/05/2020 | Full | 17.9 | 26.8 | 1.08 | 17.3 | 79 | 49 | HET1 |
| GAT20-s2 | Gatton | tSow2 | Quadrate PEM & plots | 04/08/2020 | Full | 22.2 | 31.2 | 1.35 | 19.7 | 65 | 37 | HET2 |
| WAR20-s1 | Warwick | tSow1 | Quadrate PEM & plots | 08/06/2020 | Full | 19.3 | 26.3 | 0.74 | 13.6 | 73 | 42 | HET1 |
| WAR20-s2 | Warwick | tSow2 | Quadrate PEM & plots | 12/08/2020 | Full | 23.1 | 31.4 | 1.38 | 11.6 | 53 | 39 | HET1 |

Trial identifiers indicate site (Gatton (GAT), Tosari (TOS) or Warwick (WAR)), year conducted and sowing time (tSow1 or tSow2).

tolerance in wheat (Christopher et al., 2015, 2021; Richard, 2017). In total, 35 wheat genotypes were tested in PEM and plot trials, with 32 genotypes at each trial, except for the PEM trial with quadrat harvest in 2020 when only 20 selected genotypes were used (Table S1, Supplementary). In conventional plot trials, 32 genotypes were used in each trial.

### 2.3. The photoperiod-extension method

In the novel photoperiod-extension method (PEM), LED lamps (CLA LT401, 9 W T40 LED LAMP, 3000 K 760LM) with a lumen efficiency ≥ 80 were set up at one end of each row or plot. These lights were established approximately 1 m above the ground level and at a spacing of 0.8 m. These lamps supplement light by extending the day length to 20 h (Fig. 1). The intensity of light diminishes with the square of the distance from the lights along the test row. For example, quantum flux density could decrease by 10 fold and 45 fold with 1 m and 2 m distance from the light source, respectively with minimum or no impact after 3 m (Niinemets and Keenan, 2012). The plants closest to the light could receive maximum integrated supplemental light, with minimum or no impact at the other end of the row. This variation in light intensity across the rows induced a gradient of flowering times within each genotype row / plot as the plants closest to the light developed more rapidly than the plants far from the supplemented light.

### 2.4. Plant measurements

For each PEM trial and sowing date in 2018 and 2019, approximately 20 stems of each genotype were tagged at flowering (Zadoks decimal growth stage 65; Zadoks et al., 1974). The induced gradient in phenology along the rows allowed tagging of genotypes multiple times for plants in rows or plots from each sowing time. One-to-three cohorts of stems were tagged at precisely matched flowering in rows or plots from each sowing time and trial. These sequentially tagged cohorts were termed as 'tagging 1′ (T1), 'tagging 2′ (T2) and 'tagging 3′ (T3). The spikes from tagged stems were manually harvested at maturity and processed for grain yield components.

In addition, in each test row of all PEM trials in 2018 and tSow1 trials at Tosari in 2019, a quadrat consisting of a 0.5 m section of the row that originally contained heads from tagging 1 was manually harvested to estimate yield and its components. In 2020, ~ 0.5 m section of each plot (four rows) was tagged at flowering (Zadoks 65), and a quadrat of two central rows (0.5 m each) within the tagged region was manually harvested at crop maturity.

All plots from the conventional method were harvested using a small plot machine harvester at maturity when grain moisture was approximately 11 %. Grain samples were maunally counted to calculate individual grain weight (IGW).

### 2.5. Weather conditions

Local weather stations (Campbell Scientific) were set up at each site to record weather data for each 10 min period. The light interception was measured with light sensors (Apogee SP-110 pyranometers, and Apogee SQ-110 for radiation and PAR measurements, respectively) installed at 1.5 m height. HMP60 (Vaisala INTERCAP®) probes were used to measure the air temperature (Tair) and relative humidity (RH) at 1.5 m above the ground. The environmental characteristics of each trial are presented in Table 1 and Table S2.

Thermal time was calculated in degree days (°Cd) using the following equation: (Jamieson et al., 1995)

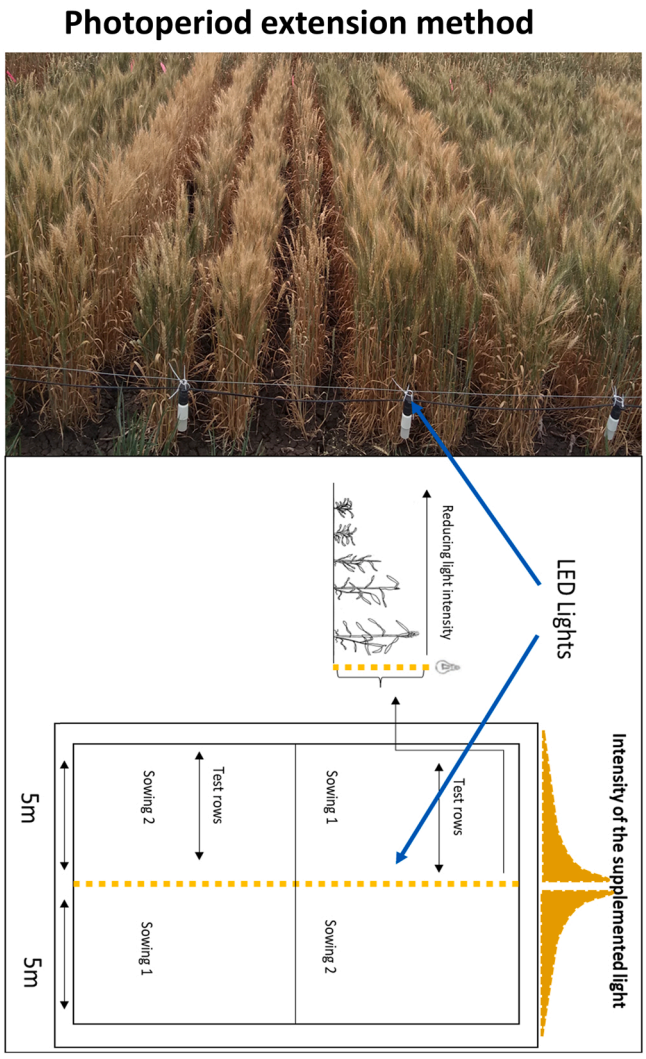


**Fig. 1.** Layout of the photoperiod-extension method (PEM). Wheat genotypes were sown either in a single row (as in this picutre) or in narrow plots of four rows. In the centre of the trial at the end of each test row, at the central axis of the trial, LED lights were setup. These supplemental lights extend the photoperiod to 20 h. The intensity of light diminishes along the row and induces a gradient of flowering times within each test row, with plants closest to the light developing faster.

$$Thermaltime = \sum_{h=1}^{24} -0.0032 * Tair_h^3 + 0.1369 * Tair_h^2 + 0.3968 * Tair + 0.993 \quad (1)$$

Where $Tair_h$ (°C) is the hourly air temperature data.

Vapour pressure deficit (VPD, kPa) was calculated hourly during the day time as in Alduchov and Eskridge (1996) by the following equation:

$$VPD = 0.61094\left(\left(\frac{1-RH}{100}\right)\right)^{17.625*Tair/(Tair+243.04)} \quad (2)$$

Where Tair (°C) and RH (%) were the hourly air temperature and hourly air relative humidity, respectively, during the daytime.

### 2.6. Statistical analysis

Data were analysed using the R4.2.0 version (R Core Team, 2018). Individual and interaction effects of genotype and environments (sowing, location and tagging) were determined by analysis of variance (ANOVA). Statistical differences were tested with student's t-tests at a 5 % level. Principal component analysis was conducted to study the correlation across different environments for IGW and grain yield of wheat genotypes and heat maps for correlations presented. The data were normalised to maximise the variance before computing the PCA. Based on their performance across different environments, wheat genotypes were ranked for IGW and grain yield and then classified into one of three groups. PCA was also used to compute the relationships among different environments.

## 3. Results

### 3.1. Wheat crops experienced a wide range of heat events across locations and sowing times

Wheat genotypes at each location, season, sowing and tagging experienced varying air temperatures and vapour pressure deficit (VPD) in the pre- and post-flowering periods (Table 1, Fig. 2 & Table S2). In all trials, plants from sowing 2 ('tSow2') experienced significantly higher temperatures and VPD than those from the first sowing ('tSow1). Post-flowering mean air temperature was ~20 % higher in tSow2 than tSow1 across all trials (Table 1). Similar differences in post-flowering daily-maximum air temperature were also observed between tSow1 and tSow2, with the exception of 2020 Warwick trial (WAR20), where temperatures were only 10 % higher. The number of hot days (with maximum temperature > 30°C) across these trials also varied greatly, with TOS19s2 in 2019 receiving the maximum number (22) of post-flowering hot days. Higher temperature during tSow2 shortened the duration of both pre- and post-flowering periods, although the reduction in time to flowering was relatively greater than the reduction in post-flowering duration across all the tested locations (Table 1).

For this study, we computed the plant response to various threshold maximum temperatures, i.e., ranging from 26 °C to 35 °C. The threshold > 30 °C value was selected as it gives the clearest separation between the genotypes under different environments. The environments with similar post-flowering stress were defined as (i) heat environment type 1 (HET1) that corresponded to environments with no or only late grain-filling heat stress (i.e. less of 4 cumulated hours of temperature > 30°C between 0 and 450°Cd after flowering), (ii) HET2 that included all environments with moderate heat stress during grain fill (5–15 days with a maximum temperature >30 °C in our set of trials), and (iii) HET3 that corresponded to environments severely stressed during grain fill (20 and 22 days with a maximum temperature >30 °C in our set of trials). In addition to post-flowering heat, HET3 trials experienced some pre-flowering high temperatures (Table S2, Supplementary), including hot days around stem elongation and meiosis (Fig. 2) that significantly reduced grain set (i.e., in GAT19 and TOS19, Table S8 Supplementary). VPD values also varied across the sowing time and locations, with late-sown (tSow2) having a relatively higher post-flowering VDP than early-sown (tSow1) crops (Fig S1). On average, GAT19-s2 and TOS19-S2 had the highest post-flowering VPD across all the tested locations and sowing times (Fig S1). There were no significant variations in the amount of hourly photosynthetic photon flux across the tested sites and sowing time in this study (Fig. S2).

### 3.2. Late-sown crops had lower individual grain weight and grain yield

Individual grain weight and grain yield varied significantly across trials, but plants typically produced significantly smaller grains and lower grain yield in tSow2 compared with tSow1 (Fig. 3). Late sown crops (tSow2) also produced significantly lower grain number than tSow1 crops except, WAR18 in PEM spike harvest and GAT20 quadrate harvest (Table S8 Supplementary), probably due to shorter pre-flowering periods associated to warmer temperatures (Table 1 & S2, Supplementary).

The maximum trial means for IGW and grain yield were measured in

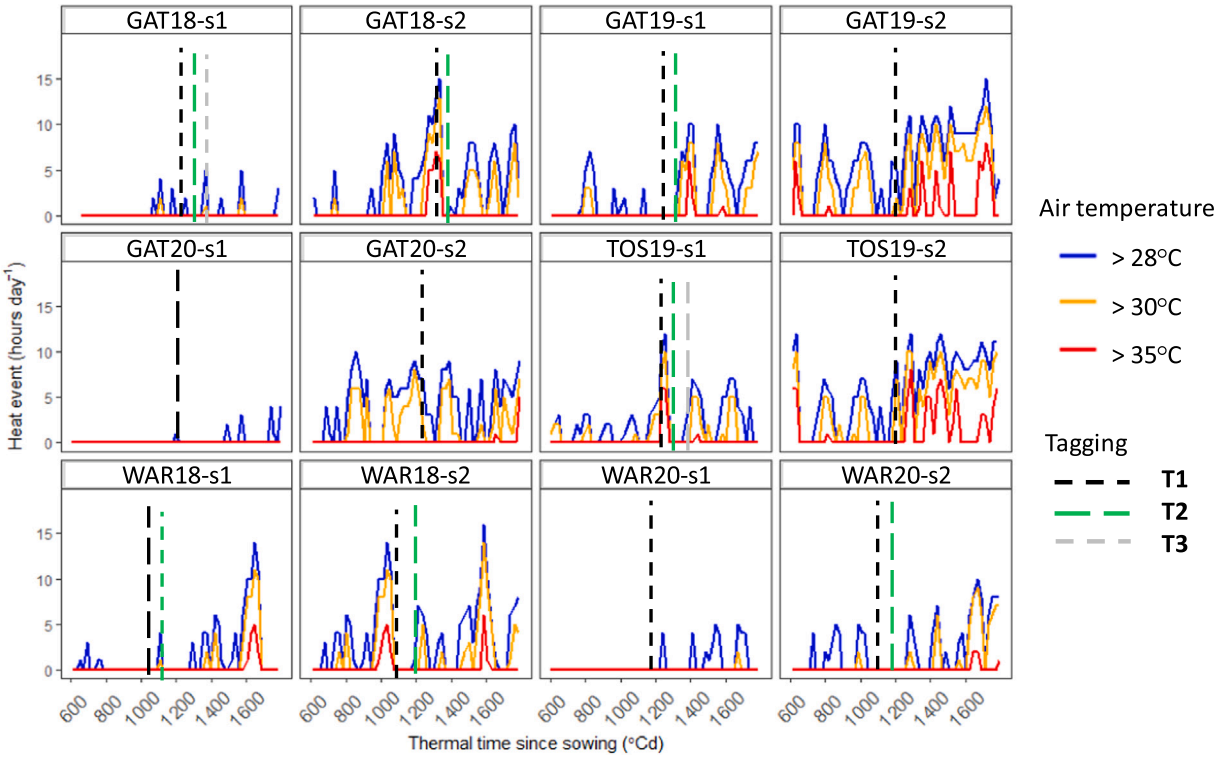


**Fig. 2.** The number of hours each day when air temperatures exceeded 26 °C (blue lines), 30 °C (orange lines) or 35 °C (red lines) is plotted against thermal time (°Cd) from sowing. These are presented for each location, season and sowing time. The vertical lines represent tagging of wheat genotypes at flowering. T1, 1st cohort of stems tagged at flowering, T2: 2nd cohort of stems tagged at flowering, T3: 3rd cohort of stems tagged at flowering. Trial identifiers are as described in Table 1. (For interpretation of the references to colour in this figure legend, the reader is referred to the web version of this article.)

HET1 environments. In the PEM with quadrat tagging and harvests, a maximum of 45.5 mg for IGW and 571 g $m^{-2}$ for grain yield was recorded in GAT18s1 (Fig. 3). With the conventional plot method, genotypes produced a maximum trial-mean IGW of 37.7 mg and a maximum grain yield of 484 g $m^{-2}$ in WAR20s1. Trial-mean reductions in IGW between tSow2 and tSow1for PEM and conventional plot trials were maximum at WAR18 (64 %) and GAT19 (47 %), respectively (Fig. 3a & b). Grain yield reduction between tSow2 and tSow1was maximum in WAR18 for the PEM and in TOS19 for conventional plots (Fig. 3c & d).

All trials were fully irrigated, except TOS19, which only received pre-flowering supplementary irrigation and was subjected to mild post-flowering drought. Given the pre-flowering conditions, tSow1 plants at TOS19 produced a high number of grains, but a significant reduction in IGW was compounded by post-flowering heat and drought (Tables S2 & S8).

### 3.3. *Extending the photoperiod allowed tagging of plants at a matched development stage from genotypes of contrasting maturity*

In the PEM trials, phenology data were collected from plants at 0.5 m at each end of each experimental row, i.e., from next to the supplemented light and from the far end away from the supplemental lights (Figs. 4 and 5). The phenology of the different genotypes significantly varied both under natural and supplemented light. Across all PEM trials, the earliest maturing genotypes flowered approximately 10.1 days (172°Cd) and 7.8 days (145°Cd) earlier than the latest maturing genotypes under natural and supplemented lights (Fig. 4). The supplemented light accelerated flowering by 7.9 days (152°Cd) and 5.4 days (114°Cd) on average in tSow1and tSow2, respectively (averaged across genotypes and trials). This gap between flowering times of plants under natural and supplemented light allowed multiple tagging of the genotypes at a matched developmental phase (Zadok 65) from a single time of sowing.

Supplemented light had a weaker effect on the phenology of late sown crops with a longer natural photoperiod than the early sown crops (Fig. 5). Under the shortest studied photoperiods (<10.5 h, at sowing), the plants closer to the lights flowered approximately 8.8 days (averaged across genotypes and trials) earlier than the plants away from the lights. The phenology effect of supplemented light was reduced by approximately 49 % on the plants sown under a relatively longer photoperiod (11.5 h or more).

### 3.4. *Individual grain weight decreased by 1.5 mg per post-flowering heat day*

Across PEM individual-spike harvests, IGW of the studied wheat genotypes was strongly correlated ($r^2 = 0.90$) with post-flowering hot days (maximum temperature >30 °C) (Fig. 6a). For example, across all the trials and tagging events, each additional post-flowering hot day (with maximum temperature >30 °C) reduced IGW by 1.5 mg as estimated from the slope of the regression (Fig. 6a). The stems receiving 0–4 post-flowering hot days (HET1) produced the heaviest grains (40–45 mg) in this study (Fig. 6a). In contrast, moderately stressed stems, with 5 and 15 post-flowering hot days (HET2), had a significantly lower mean IGW and total grain weight per spike than those in HET1 (Fig. 6). The most stressed stems (post-flowering hot days > 15) were grouped under HET3 (Fig. 3). For example, In GAT19s2 and TOS19s2, the plants experienced 20 and 22 post-flowering hot days, respectively, and experienced maximum IGW loss. On average, stems under these extremely hot conditions produced 2.7 times lighter grains than the potential IGW (Fig. 6a).

While the greatest environmental variations occurred between sites and sowings, variations in the number of hot days and mean IGW were also observed among stems tagged at different times (i.e., a group of stems flowering at different dates) within a single sowing time. For instance, T2 stems of GAT19s1 produced 14 % smaller grains than T1

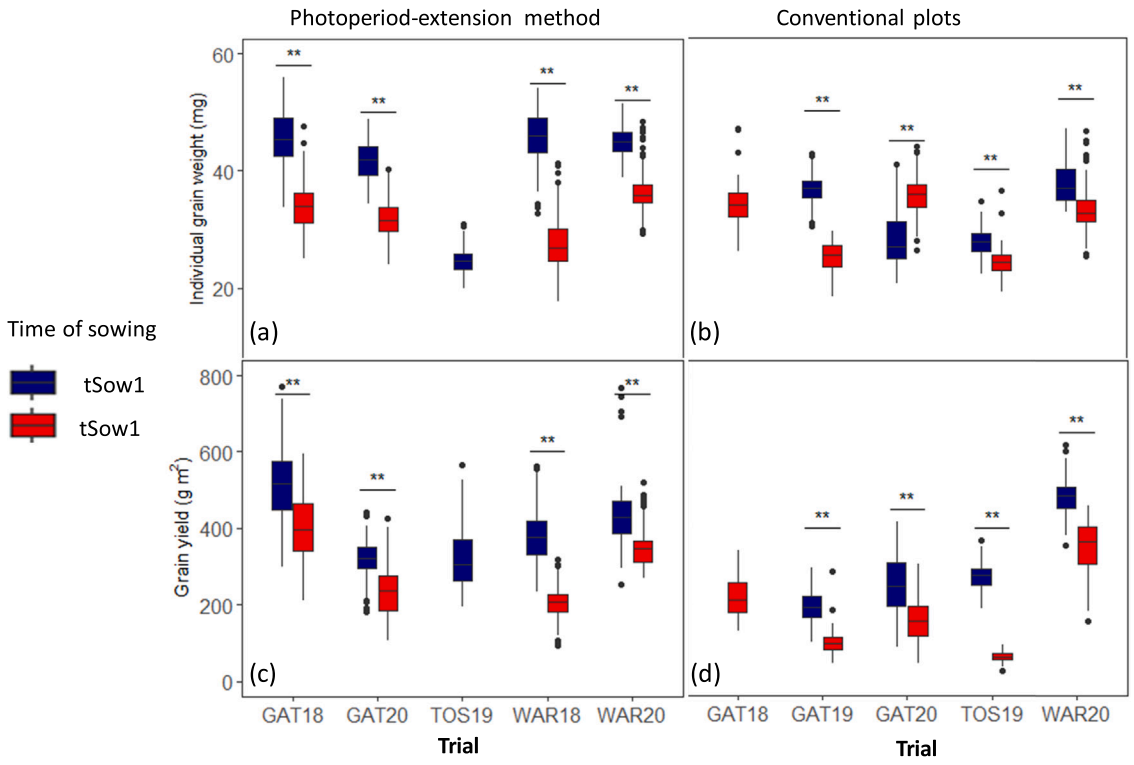


**Fig. 3.** Effect of sowing time on (a, b) individual grain weight and (c, d) grain yield of tested wheat genotypes for trials with (b, d) conventional plots or (a, b) the photoperiod-extension method with quadrat tagging and harvests. Each boxplot displays data from 32 genotypes and four independent replicates. TOS19 crops only had supplementary irrigation and experienced mild post-flowering water stress. In the boxplot, horizontal black lines inside each box denote median values; boxes extend from the 25$^{th}$ to the 75$^{th}$ percentile of each group's distribution of values; the whiskers are the 10$^{th}$ and 90$^{th}$ percentiles; and the dots outside the whiskers represent individual values outside this range. ** corresponds to significant differences at $P < 0.001$ between the two sowing times within each trial. In 2018, tSows2 plots were established only at Gatton (GAT18) and in 2019, quadrat harvests were taken from the tSow1PEM trials at Tosari (TOS19) only. Trial identifiers are as described in Table 1.

stems (Fig. 6a, Table S3).

### 3.5. The photoperiod-extension method provided a stable genotype ranking within heat environment types

In this study, PEM-based genotypic rankings for IGW were relatively more consistent for the environments experiencing a similar number of post-flowering hot days than the ranking assessed in conventional plots (Fig. 7). For single spike harvests with PEM, IGW correlations for stems experiencing mild or no heat stress during grain-filling (HET1), ranged from *r* of 0.64–0.89 (Fig. 7a). In HET2, *r* correlations ranged from 0.2 to 0.90 for fully-irrigated trials (i.e. all trials except TOS19 which experienced a post-flowering drought). These correlations were stronger (0.57–0.9) among the irrigated trials with a similar number of hot days (i.e. 9–13) and became more variable with the environment (GAT19s1T1) with five hot days only (*r* of 0.2–0.57). IGW of the two severely-stressed environments (HET3) were strongly correlated ($r = 0.46$, Fig. 7a). Correlations between HET1, HET2 and HET3 varied, with moderate to high correlations between HET1 and HET2 environments and weaker correlations with HET3 environments.

IGW from PEM quadrat harvests were also positively correlated between the different tested environments, and these correlations were particularly strong among environments experiencing a similar number of hot days (Fig. 7b). For example, in HET1, these correlations were moderate to strong (*r* of 0.24–0.88) mainly because of a weaker correlation between GAT20s1 and WAR20s1 ($r = 0.24$). Similarly, all fully-irrigated HET2 environments were positively correlated, with correlations ranging from 0.19 to 0.68.

In the conventional plot trials, genotype ranking for IGW varied widely across environments, both between sowings and sites (Fig. 7c). Correlations between non-stressed environments (HET1) were relatively high (*r* of 0.4–0.78). However, correlations between HET2 environments were highly variable or even negative (*r* of −0.15 to 0.42). Similarly, HET3 trials GAT19s2 and TOS19s2 had a correlation of 0.10.

Grain yield from PEM quadrat harvests for irrigated trials was also positively correlated. The correlations ranged from 0.18 to 0.72 within HET1, and from 0.33 to 0.63 within HET2 (Fig. S4b, supplementary data). In contrast, for conventional plots, correlations for grain yield were either poor or negative for most trials, irrespective of their heat environment types (Fig. 7c). For instance, maximum correlations within HET1, HET2 and HET3 were 0.3, 0.21 and − 0.36, respectively.

Genotype rankings were also compared across the different methods used in this study. Strong positive relationships ($r^2$ from 0.65 to 0.97 depending on the environment considered) were observed between the IGW from PEM trials with (i) individual spike harvest and (ii) quadrat harvest under fully irrigated conditions (Fig. 8a). In contrast, correlations for IGW between PEM quadrat harvest and conventional plot trials under irrigated conditions were not as close in most trials ($r^2$ from 0.19 to 0.57; Fig. 8b).

### 3.6. The photoperiod-extension method allowed genotypes to be discriminated according to their performance in different heat environments types

Performance of wheat genotypes in terms of IGW and total grain weight were analysed using a principal component analysis (PCA, Figs. 9 & 10). The first two principal components (PC) combined explained more than 50 % variance across environments in both IGW and grain yield for all the tested methods, except for grain yield in conventional field plots (Fig. 10).

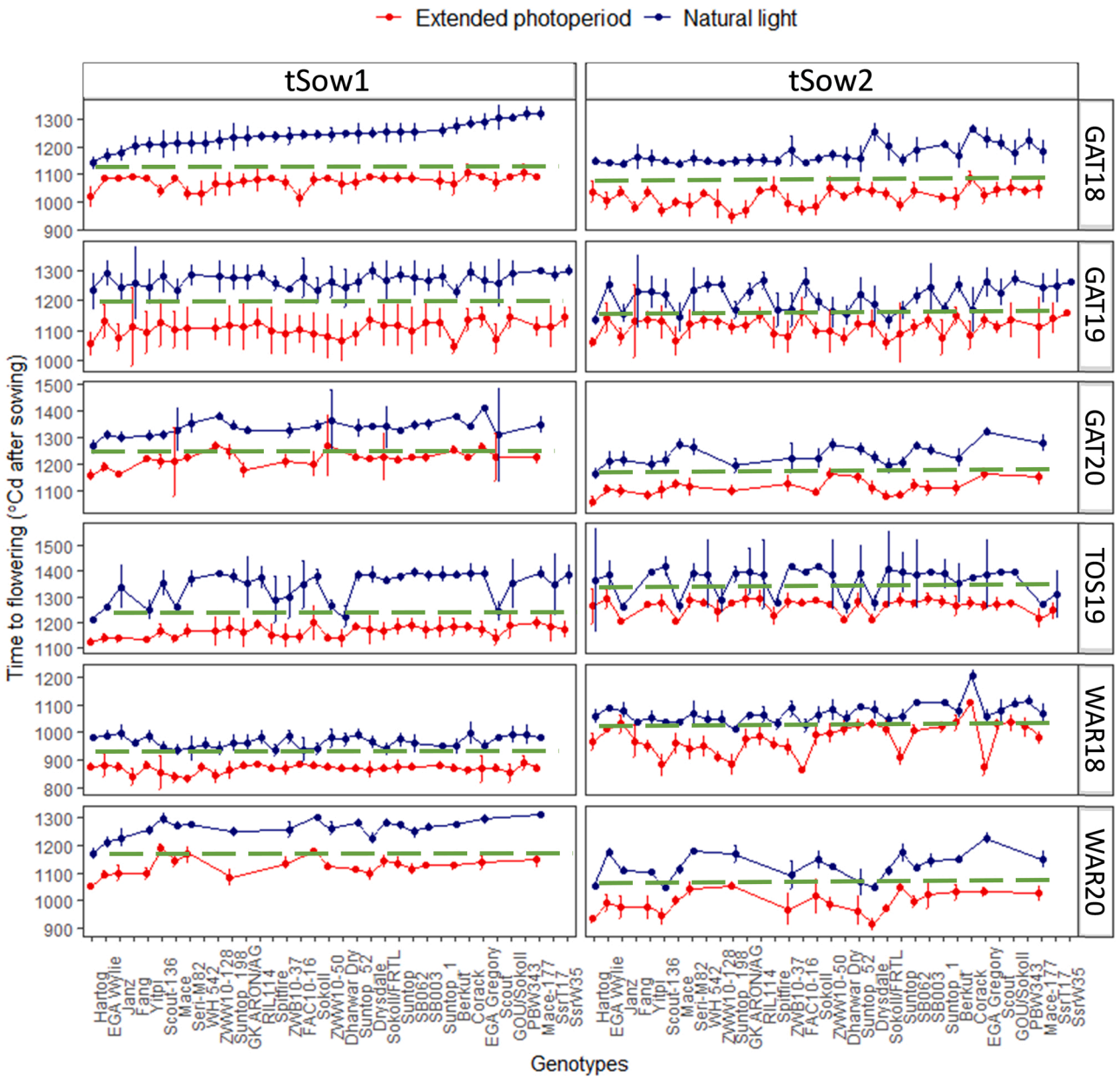


**Fig. 4.** Flowering time of wheat genotypes with and without supplemented light. Horizontal dashed lines correspond to the day of tagging of all wheat genotypes at matched flowering. Data on flowering were collected for plants 0.5 m away from the light source (extended photoperiod, red) and plants 0.5 m from the end of the row (natural light, blue). Values correspond to the mean of four independent replicates ± confidence interval (95 %). tSow1and tSow2 represent sowing 1 and sowing 2, respectively. (For interpretation of the references to colour in this figure legend, the reader is referred to the web version of this article.)

For PEM spike harvests, strong positive correlations were observed between fully-irrigated HET1 and HET2 environments, as indicated by the small angles between the vectors in the biplots (Figs. 9a & 10a). These correlations were stronger within HETs for IGW (Fig. 9a) than for total grain weight per spike (Fig. 10a). In contrast, a wider angle between vectors for HET3 and HET1-HET2 suggested weaker correlations between these environments (Figs. 9a & 10 a). Drought affected TOS19s1, which also experienced moderate post-flowering heat stress (HET2), more closely correlated with HET3 environments severely stressed by heat both for IGW and total grain weight per spike.

The projection of a genotype onto an environmental axis reflects the performance of that genotype in that environment. Genotypes were grouped based on their performance in environments from the PEM spike harvests. Biplots separated genotypes into three distinct groups for IGW (Fig. 9) and three partly differentiated groups for grain weight per spike (Fig. 10). Top performing genotypes in HET1 and HET2, such as ZWB10–37 (in green in Figs. 9 & 10) project above the origin on axes corresponding to HET1 and HET2. In contrast, poorly performing genotypes such as Yitpi and EGA Wylie (in red in Fig. 9 & 10) project below the origin on the same axes. The top and poor performing genotypes identified with the PEM spike harvests were consistent with those identified from the PEM quadrat harvests data (Figs. 9b & 10 b).

For the conventional plots, heat environment types (HET) were less clearly differentiated, particularly for grain yield, indicating less power to distinguish between HETs (Figs. 9c & 10 c). Genotype rankings were also changed compared to ranking with the PEM. For instance, Suntop_1 ranked among the top performing genotypes for IGW in HET1 and HET2 in the conventional plot trials (Fig. 9c) but it ranked with the intermediate to poor group with the PEM (Fig. 9a). For grain yield in conventional plot trials, genotype performance was even more difficult to differentiate. For example, top performing genotypes in the PEM (in green) were not distinct from others in conventional plots being

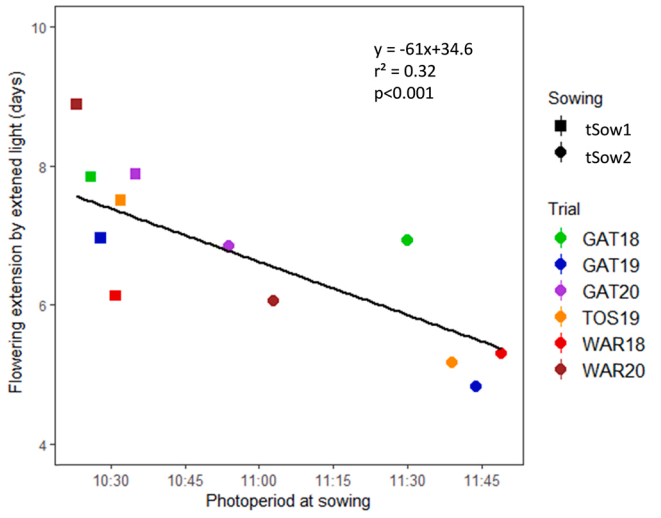


**Fig. 5.** Delay in flowering time due to supplemented light in response to the photoperiod measured at sowing in all trials and sowings. The delay in flowering was calculated as the difference in flowering dates for plants located 0.5 m (i.e. extended light, 20 h) and 4.5 m (i.e. natural light) away from the lights. Data correspond to the mean of 32 (2018 and 2019) or 20 (2020) genotypes and four independent replicates for all PEM plots. TOS19 crops only had supplementary irrigation and experienced mild post-flowering water stress.

scattered almost randomly across the biplot (Fig. 10c).

## 4. Discussion

### 4.1. A new method to screen for heat tolerance at matched development stages

During both the reproductive and the grain filling phases, the sensitivity of developing grains to heat events can change over a period as short as a few days (Stone and Nicolas, 1995; Chenu and Oudin, 2019). Since field-based techniques for screening heat tolerant germplasm generally rely on different sowing times, it is hard to optimise sowing time given the unpredictable timing of heat events. Field-based screening for heat tolerance using this conventional method is further complicated when genotypes with varying maturity types are tested together. These genotypes are likely to be at different developmental stages when natural heat events occur. Thus, heat escape at a less sensitive stage can confound comparisons of heat tolerance, per se.

We developed a new method using supplemental lights to screen heat tolerance of wheat genotypes at matched developmental phases. Light-induced phenology manipulation to synchronised flowering had previously been proposed to study the post-heading response of wheat and barley germplasm (Frederiks et al., 2012). In our new method, the photoperiod was extended to 20 h at one end of test rows of plots. The light intensity diminishes with the square of the distance (Niinemets and Keenan, 2012), generating a gradient of flowering times along the length of the test rows (Figs. 1 & 4). The range of flowering times within a single row of individual genotypes, allowed a comparison of the performance of genotypes with varying maturity types at matched developmental stages. The method was tested for sowing dates from late May to mid-September. The impact of extended photoperiod on flowering was associated with the natural photoperiod during vegetative crop growth ($r^2 = 0.32$; Fig. 5). A wide gap in flowering along the rows, of up to 8.8 days when averaged across all tested genotypes, was recorded when planting under short photoperiod (<10.50 h). This gap narrowed by 3.5 days with each increasing hour in photoperiod at later sowing dates (Fig. 5) so that all genotypes flowered within only 4.5 days of each other in the latest sowing dates tested. A wider flowering-time gradient is interesting as it allows; (i) multiple taggings within a single time of sowing, which may increase the probability of being able to screen for heat at a particular stage, (ii) more flexibility for operators to visit the trial during the appropriate window and tag all genotypes at a matched development stage, and/or (iii) a wider range of maturity types to be considered. Despite this additional flexibility, the robust genotype rankings generated with the PEM suggest that a single tagging is likely sufficient for reliable screening.

In the conditions tested, sowing dates for screening post-flowering heat tolerance between early July and late August provided the best discrimination. Sowings during this period were typically associated with moderate post-flowering heat stress (HET2) and a relatively wide flowering gradient for tagging stems or quadrats at a matched development stage. With earlier sowings, very few heat events occurred. In contrast, later sowings had a narrower flowering gradient and a greater risk of exposure to a high number of severe heat events, which can increase heat damage to a level where variation between genotypes is

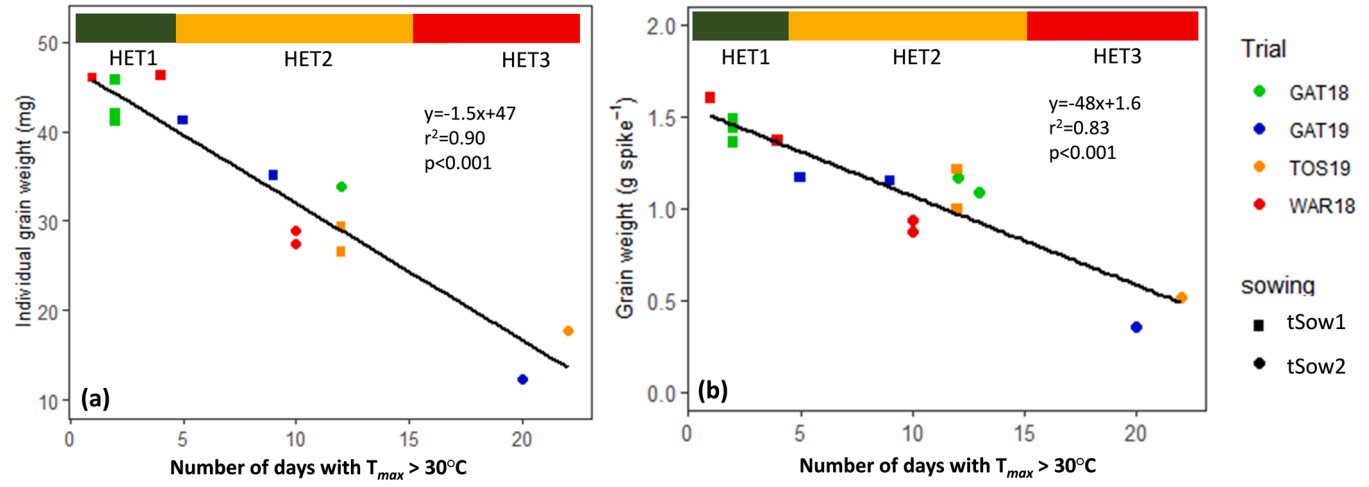


**Fig. 6.** Changes in (a) individual grain weight and (b) spike grain weight in response to the number of post-flowering hot days with a maximum temperature ($T_{max}$) > 30 °C during the period from 0 to 500°Cd after flowering (Number of days >30 °C) across locations and sowing times. Each point represents the mean of all genotypes for individual grain weight of spikes that flowered the same day (four independent replicates of 20 stems each). Different tagging events within each trial and sowing time are represented by points with the same colour. Heat environment types are indicated by the horizontal bar at the top of each panel (HET1, green; HET2, orange; HET3, red). TOS19 only had supplementary irrigation and experienced mild post-flowering water stress. (For interpretation of the references to colour in this figure legend, the reader is referred to the web version of this article.)

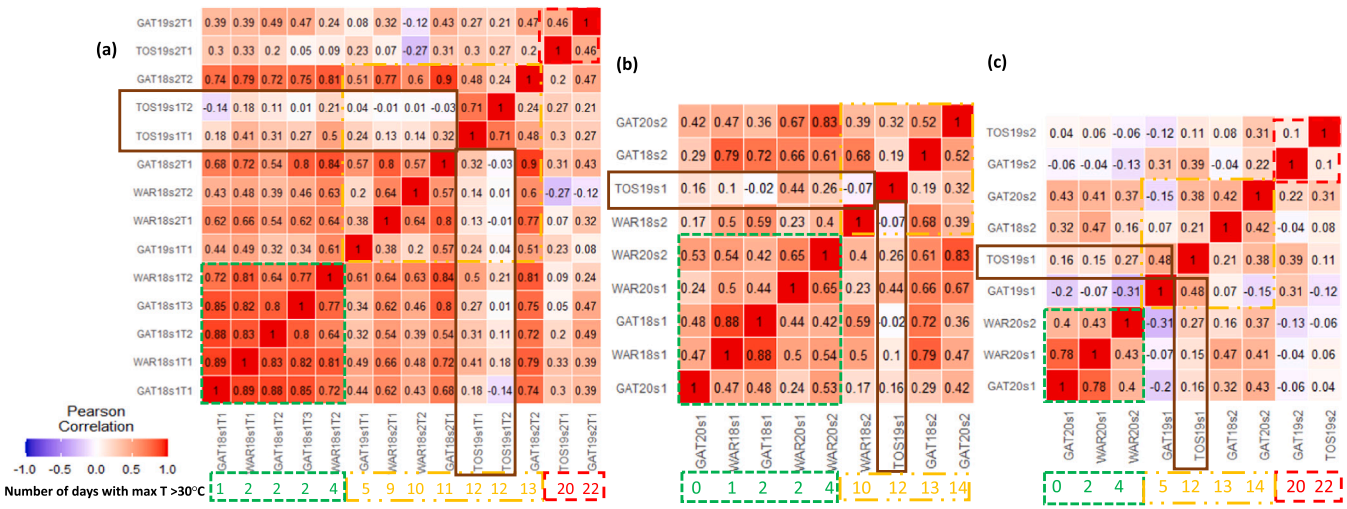


**Fig. 7.** Genetic Pearson's correlation coefficients (r) for individual grain weight between environments. Correlations for mean individual grain weight of genotypes between each pair of tested environments (i.e. site x year x sowing x tagging-event combinations). Individual grain weight was estimated from measurements at (a) spike level and at (b) crop level with quadrat harvests in the photoperiod-extension method (PEM), as well as at (c) the plot level in the conventional plot trials. Below the heat maps are indicated the number of post-flowering hot days with maxima exceeding 30 °C from 0 to 500°Cd after flowering for each environment, grouped by heat environment types indicated by dashed, coloured boxes (HET1, green; HET2, orange; HET3, red). All environments were fully irrigated except TOS19 (framed in brown), which experienced mild post-flowering water stress. Genetic correlations for total grain weight are presented in Fig. S4. (For interpretation of the references to colour in this figure legend, the reader is referred to the web version of this article.)

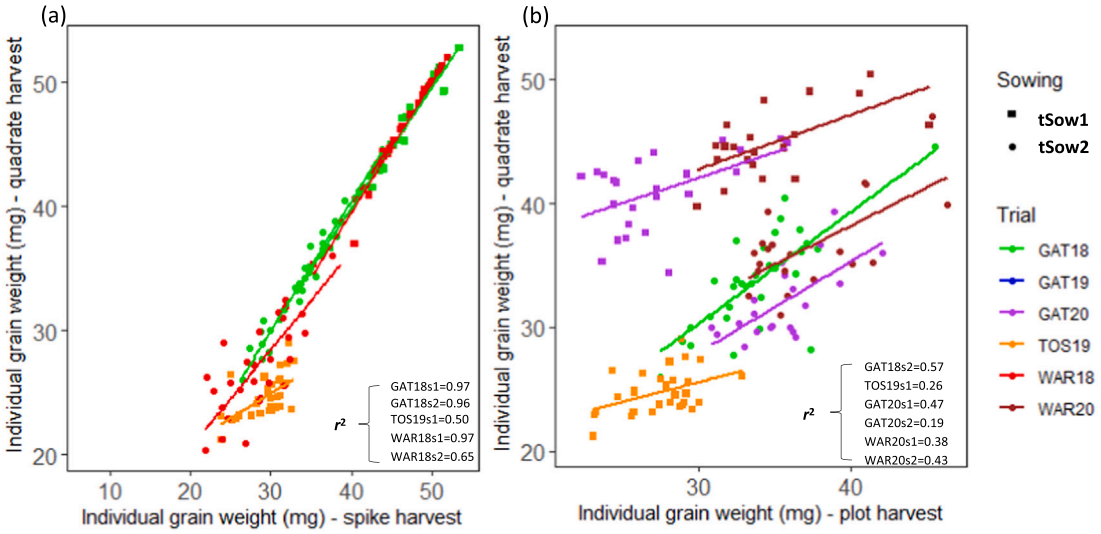


**Fig. 8.** Correlations for individual grain weight of all studied genotypes between either (a) data collected from individually tagged stems and tagged quadrats at the matched development stage with the photoperiod-extension method (PEM) or between (b) the PEM with quadrat tagging and harvests and conventional plots. Each data point represents the genotypic mean value of four independent replicates. Correlations for total grain weight are presented in Fig. S3.

reduced. Late sowings are also usually more prone to pre-flowering heat (e.g. TOS19s2 and GAT19s2), thus resulting in confounding effects, with IGW varying due to both a decrease in grain number and direct effects of post-flowering heat stress. Optimum sowing dates to screen heat stress obviously depend on the targeted stress (e.g. with or without pre-flowering heat). They also depend on the test location that impacts both wheat phenology and the frequency of heat events. Crop models can help identify locations and sowing windows for efficient heat tolerance screening in particular target environments (e.g. Chauhan et al., 2017; Chenu et al., 2017; Collins et al., 2021).

### *4.2. The PEM method allows reliable ranking of wheat genotypes under varying environments*

The observed strong correlations among trials for either IGW or grain yield with PEM than conventional plots in this study (Figs. 7a & b, S4a & b) suggest that a stable ranking of tested genotypes, particularly within the environments receiving a similar degree of heat ((Supplementary Tables S4, S5 & S7). For instance, for the PEM with individual-spike harvests, the respective mean *r* correlations within fully-irrigated HET1, HET2 and HET3 environments were 0.80, 0.59 and 0.46 for IGW; and 0.75, 0.54 and 0.57 for total grain weight per spike. In contrast, these correlations were typically much weaker in conventional plots with *r* averages of 0.53, 0.11 and 0.1 for IGW, and 0.05, 0.12 and − 0.36 for grain yield within HET1, HET2 and HET3, respectively (Figs. 7c, S4c, Supplementary Tables S6 & S8). This indicates that in conventional plots, the ranking of wheat genotypes was highly variable depending on environmental conditions, including for the targeted moderate grain-filling heat stress (HET2).

The PEM allowed the tested genotypes to be clustered into distinct

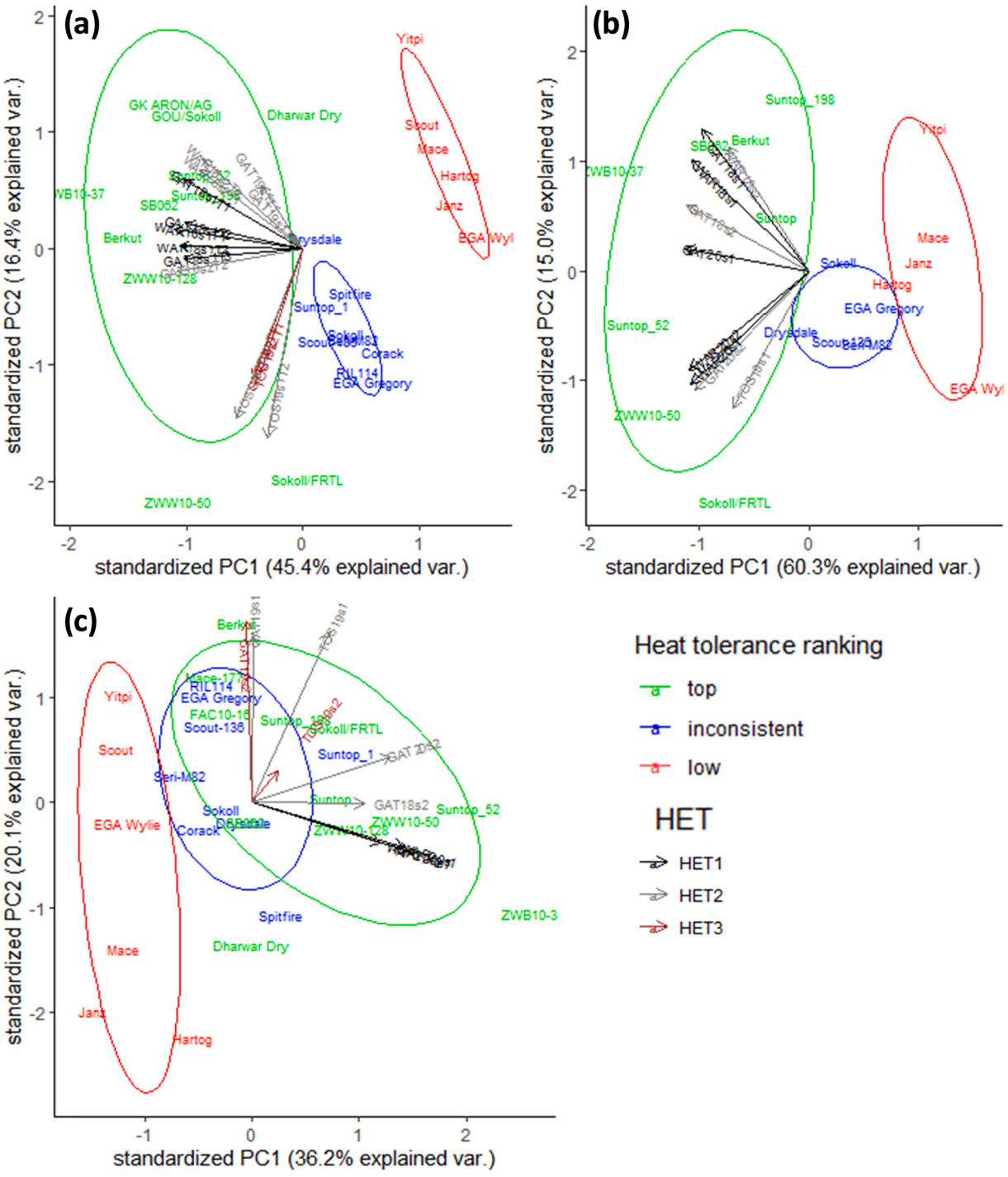


**Fig. 9.** Principal component analysis biplots of individual grain weight (IGW) of studied wheat genotypes for the PEM spike harvests (a), PEM quadrat harvests (b) and conventional machine harvested plot trials (c). Environments corresponded to combinations of sowing dates, sites and years together with tagging events for single-spike harvests (a). Principal component loadings (arrows) were coloured and grouped based on heat environment type (HET); HET1, black; HET2, grey; HET3, brown. Genotypes were grouped for similarity in their performance for either IGW, i.e. green, top performing genotypes in HET1 and HET2, blue, genotypes with inconsistent / poor performance, particularly across HET1 and HET2; red, genotypes with poor performance across most tested environments. Eclipse colours correspond to the performance groups for genotypes. (For interpretation of the references to colour in this figure legend, the reader is referred to the web version of this article.)

groups based on their performance in these environments (Figs. 9a, b & 10a, b). In contrast, this genotype clustering was inconsistent with that found in conventional plots. The clustering in the conventional plots was also much less powerful at separating groups of genotypes, as seen by the greater overlap of genotypes within each group (Figs. 9c & 10 c). This indicates that the PEM ranked wheat genotypes more consistently across a wide range of heat-stressed environments compared to conventional plot trials. It may be important to note, however, that in manipulating flowering time to different extents depending on the maturity types of the genotypes, other traits associated with phenology such as source-sink relationships may also be affected. For instance, phenology acceleration in some genotypes may reduce their assimilate

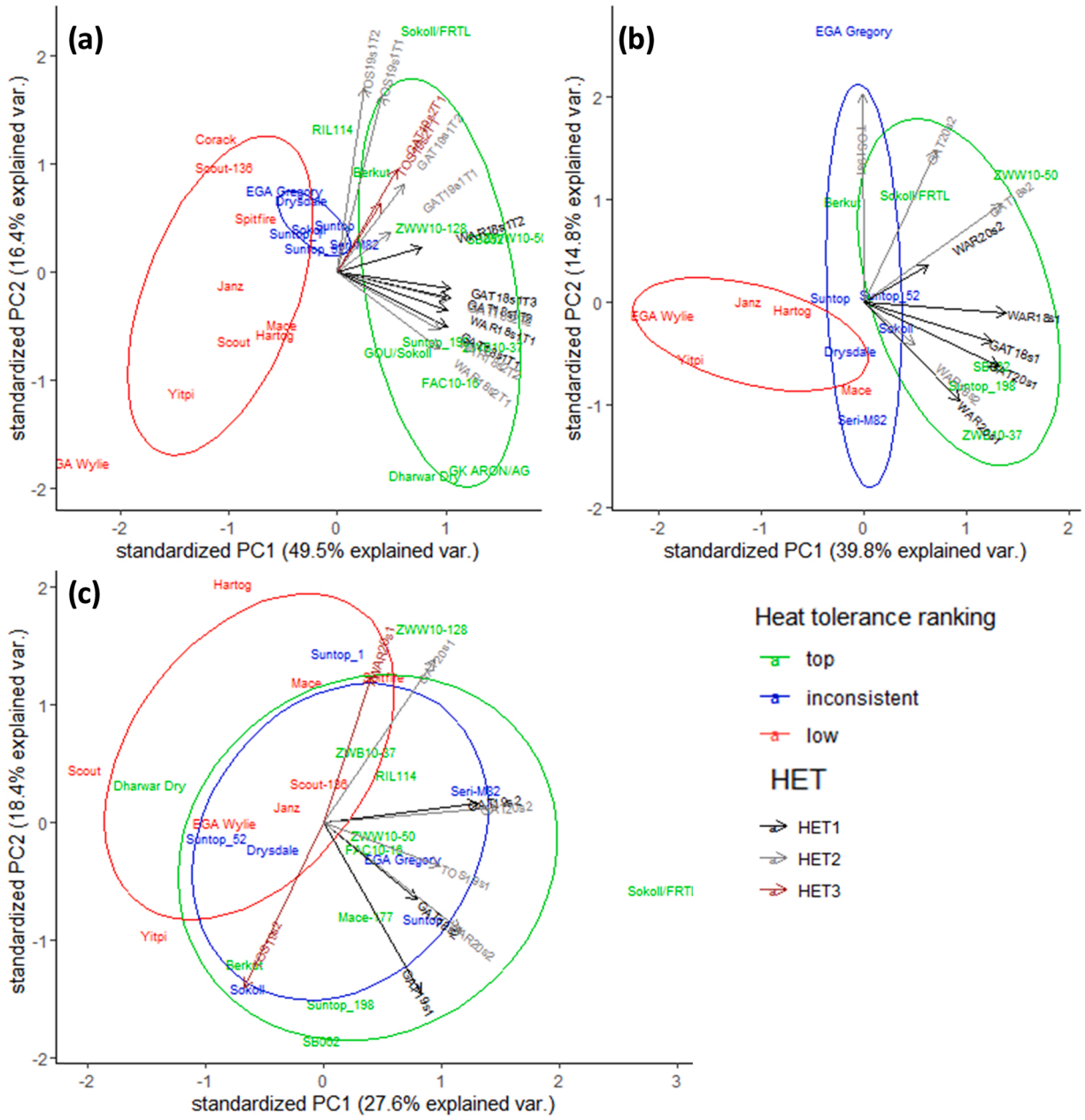


**Fig. 10.** Principal component analysis biplots of (a) grain weight per spike or (b-c) grain yield of studied wheat genotypes for the PEM spike harvests (a), PEM quadrat harvests (b) and conventional machine harvested plot trials (c). Environments corresponded to combinations of sowing dates, sites and years together with tagging events for single-spike harvests (a). Principal component loadings (arrows) were coloured and grouped based on heat environment type (HET); HET1, black; HET2, grey; HET3, brown. Genotypes were grouped for similarity in their performance for either grain weight per spike (a) in PEM spike harvests or total grain weight (b-c) in PEM quadrate and conventional plots, i.e. green, top performing genotypes in HET1 and HET2, blue, genotypes with inconsistent / poor performance, particularly across HET1 and HET2; red, genotypes with poor performance across most tested environments. Eclipse colours correspond to the performance groups for genotypes. (For interpretation of the references to colour in this figure legend, the reader is referred to the web version of this article.)

storage in stem tissues (Rebetzke et al., 2008), post-flowering remobilisation capacity, and ultimately response to heat. Nevertheless, in the current study, genotype ranking was found highly consistent within HET over a large range of flowering times, suggesting that heat was a major driver in the observed phenotypes.

### *4.3. The PEM provided new insights into the impact of post-flowering heat events on individual grain weight and yield during naturally occurring heat events in the field*

The PEM allowed estimation of the effects of heat stress in the field while largely removing potentially confounding effects from differences in phenology between genotypes allowing more reliable ranking of genotypes responses to heat stress in different environments. Crop simulation studies identified post-flowering heat as the major determinant of wheat productivity in the Australian Wheatbelt for current and future climates (Ababaei and Chenu, 2020; Collins and Chenu, 2021). Data from the current study demonstrate experimentally how heat intensity during the grain filling period is a major determinant for IGW and grain yield in irrigated field conditions (Fig. 6). In the field conditions tested in the current study, each additional hot day during grain filling reduced IGW by 1.5 mg (Fig. 6a). This significant ($p < 0.001$) reduction in IGW was also found in plants sown at a single date but exposed to a range of natural heat events.

Earlier field-based studies showed significant damage to wheat crops under post-flowering heat (Gebeyehou et al., 1982; Gerard et al., 2020; Telfer et al., 2018; Thistlethwaite et al., 2015). However, with the conventional field-based screening, it is hard to accurately quantify the impact of natural heat events on the wheat genotypes with varying phenology. For example, wheat grain yield loss is often associated with post-flowering maximum temperature $> 30\,^{\circ}C$ (Porter and Gawith, 1999; Girousse et al., 2021) for the whole post-flowering period (Thistlethwaite et al., 2015, 2020). In the tested fully irrigated conditions with PEM, wheat genotypes did not experience any significant IGW or grain yield loss under 0–4 hot days (maximum daily temperature $> 30^{\circ}C$) during grain filling (HET1, Fig. 6a). Our study shows that wheat crops may not suffer any significant grain yield loss when heat events are either brief (1–2 h only) or occur late during crop development, when grain filling was already well advanced i.e. $> 450^{\circ}Cd$ after flowering (Fig. 2). This highlights the importance of estimating the developmental phase specific heat, instead for the whole grain filling period. A significant and strong effect of the timing of heat stress has also been recorded for wheat IGW during early to mid grain filling under controlled environments (Stone and Nicolas, 1995). They also suggested that the impact of heat on wheat grain weight diminishes as grain development progresses. Thus heat-induced grain yield loss should be estimated for the specific developmental crop phases.

Under a conventional field, where the impact of heat is generally calculated for the whole grain filing phase, estimated grain yield loss may significantly vary with the timing of heat stress (Thistlethwaite et al., 2020). For example, in GAT19s1, stems tagged one week apart (taggings 1 & 2) experienced different levels of heat stress, with stems from tagging 2 being subjected to four additional days of post-flowering heat and producing grain 14 % lighter than stems from tagging 1 (Fig. 6a, Table S3).

### 4.4. Implications for breeding

A high-throughput and accurate method for screening heat tolerance is necessary for sustaining food security under changing environments, particularly for projected hot and dry environments (Collins and Chenu, 2021). The PEM was tested using single rows (hand planted) and small plots (machine planted) with tagging of either individual stems or small quadrats at distances from the lights where development was matched at the flowering stage. The most reliable genotype ranking was achieved by tagging and harvesting individual spikes (Figs. 7a, 9a & 10 a, S4a). However, strong positive relationships for either IGW ($r^2$ from 0.65 to 0.97) or total grain weight ($r^2$ from 0.34 to 0.97 across environments) between individual-spike and quadrat harvests were observed for the PEM (Figs. 8a & S3), suggesting that reliable screening may be done with the PEM for small plots with quadrat harvest. This was supported by the results, as genotype ranking with quadrat harvest was also robust (Figs. 7b, 9b & e, S3b) with strong genetic correlations between tested environments (average $r$ of 0.51 in HET1 and 0.53 in HET2 for IGW, and 0.47 and 0.36 for grain yield). Using the PEM, with genotypes sown in small plots with machinery and harvested from plot segments tagged at a matched developmental stage, could have great potential to be scaled up for a large number of genotypes. However, the PEM spike harvest is most likely to be useful for identifying new sources and mechanisms of heat tolerance as well as to screen smaller of elite lines in late stages of breeding programs.

In the tested conditions, the PEM allowed effective screening for post-flowering heat stress (HET2), which is the main type of heat stress targeted for Australian production regions in current and projected climates (Collins and Chenu, 2021). A robust screening was also performed for non-stressed environments (HET1) and severely stressed environments (HET3) that happened to be affected by both pre- and post-flowering heat in the tested conditions. Different genotype rankings were observed between heat environment types HET2 and HET3, highlighting the importance of screening in the relevant target HET. The occurrence of water stress also strongly impacted genotype ranking (e.g. Figs. 2 and S3), suggesting that heat and drought adaptations are at least partly regulated by different processes. This highlights the importance of understanding the physiology and genetics associated with heat tolerance, drought tolerance and their interaction.

The PEM described here offers an opportunity to select heat tolerant wheat genotypes more reliably than can be done conventionally. We anticipate that the cost of using the PEM will be less than some other specialist methods to measure heat stress in the field. For example, the field heat chamber method requires construction of specialist chambers and the expense of fuel for regulating in-chamber temperature / relative humidity. Further, these chambers need frequent installation and removal as the genotypes achieve specific developmental stage, which increases the operational cost. In contrast the PEM uses standard equipment while requiring less labour for installation and maintenance. For the current study, each LED lamps costs ~A$5.0 (initial cost) with an on-going 9 Watts / hour power consumption. The cost of building and running PEM in the field may vary with the location but generally it is significantly lower than running air conditioners in the specialist chambers.

This method could also be adjusted and deployed in other regions and crops, with sowing dates adapted to the targeted heat environment type. However, for open pollinated indeterminate crops such as canola and sunflower, where flexibility of flowering times allows screening of genotypes across multiple developmental phases, this method might have a limited applicability. Under our studied environments, PEM was more effective for the crops sown during the shorter photoperiods and it may not be less effective for summer crops e.g. sorghum and rice. At this point, our developed PEM using only simple LED lights of lumen efficiency $\geq 80$, and by adjusting light intensity / wavelengths it may also work for the crops grown under photoperiods.

## 5. Conclusions

A new field-based method was developed and tested to screen wheat genotypes for post-flowering heat tolerance under natural heat events. In this method, supplemental light was used to manipulate crop phenology in a way that allowed genotypes with varying phenology to be tested at a closely matched developmental stage when a heat event occurred. IGW of wheat genotypes tested in this study was highly sensitive to the number of hot days during early-to-mid grain filling, particularly in the most relevant heat environment for Australian wheat crops (HET2). Clustering of genotypes across tested environments with a PCA further highlighted the ability of the PEM to differentiate genotypes based on their performance in similar heat-stress environments. In contrast, rankings were substantially changed between environments with moderate (HET2) and severe (HET3) heat stress. Similarly, genotype rankings greatly varied between fully-irrigated HET2 environments and HET2 environments subjected to post-flowering water stress.

With the increasing frequency of post-flowering heat stress affecting wheat growing regions, the photoperiod-extension method promises to improve the efficiency of heat tolerance field screening, particularly when comparing genotypes of different maturity types. However, this method could be further optimised for scaled up screening as well as for the crops different photoperiod requirements.

## CRediT authorship contribution statement

**Najeeb Ullah:** Conceptualization, Methodology, initial draft development. **Karine Chenu:** Conceptualization, data analysis, Reviewing and Editing. **Troy Frederiks:** Conceptualization, data collection. **Jack Christopher:** Data curation, Reviewing and Editing. **Shangyu Ma:** data collection, Investigation. **Daniel KY Tan:** Conceptualization, Reviewing and Editing.

## Declaration of Competing Interest

The authors declare that they have no known competing financial interests or personal relationships that could have appeared to influence the work reported in this paper.

## Data availability

Data will be made available on request.

## Acknowledgements

The research was made possible thanks to the support of The University of Queensland and the Queensland Government, Department of Agriculture and Fisheries. Najeeb Ullah was supported by a Queensland Government, Advance Queensland Fellowship. We acknowledge the assistance of Ian Broad (Department of Agriculture and Fisheries Queensland) with operating of weather stations across the studied sites, Brian Collins (James Cook University) for data analysis and Thaís Helena Godoy Sanches for sample processing and data collection.

## Appendix A. Supporting information

Supplementary data associated with this article can be found in the online version at doi:10.1016/j.eja.2023.126757.

## References

Ababaei, B., Chenu, K., 2020. Heat shocks increasingly impede grain filling but have little effect on grain setting across the Australian wheatbelt. Agric. . Meteorol. 284, 107889 https://doi.org/10.1016/j.agrformet.2019.107889.

Alduchov, O.A., Eskridge, R.E., 1996. Improved Magnus form approximation of saturation vapor pressure. J. Appl. Meteorol. 35 (4), 601–609. https://doi.org/10.1175/1520-0450(1996)035<0601:IMFAOS>2.0.CO;2.

Bennett, D., Reynolds, M., Mullan, D., Izanloo, A., Kuchel, H., Langridge, P., Schnurbusch, T., 2012. Detection of two major grain yield QTL in bread wheat (Triticum aestivum L.) under heat, drought and high yield potential environments. Theor. Appl. Genet. 125, 1473–1485. https://doi.org/10.1007/s00122-012-1927-2.

Chapman, S.C., Chakraborty, S., Dreccer, M.F., Howden, S.M., 2012. Plant adaptation to climate changeopportunities and priorities in breeding. In: Crop and Pasture Science, 63, 251–268. ⟨https://doi.org/10.1071/CP11303⟩.

Chauhan, Y., Allard, S., Williams, R., Williams, B., Mundree, S., Chenu, K., Rachaputi, N. C., 2017. Characterisation of chickpea cropping systems in Australia for major abiotic production constraints. F. Crop. Res. 204, 120–134. https://doi.org/10.1016/j.fcr.2017.01.008.

Chenu, K., Oudin, F., 2019. Heat Impact on Yield Components of Fertile Primary Tillers in Wheat Can Inform Crop Modelling for Future Climates, 23–26.

Chenu, K., Porter, J.R., Martre, P., Basso, B., Chapman, S.C., Ewert, F., Bindi, M., Asseng, S., 2017. Contribution of crop models to adaptation in wheat. Trends Plant Sci. 22, 472–490. https://doi.org/10.1016/j.tplants.2017.02.003.

Christopher, J., Richard, C., Chenu, K., Christopher, M., Borrell, A., Hickey, L., 2015. Integrating rapid phenotyping and speed breeding to improve stay-green and root adaptation of wheat in changing, water-limited, australian environments. Procedia Environ. Sci. 29, 175–176. https://doi.org/10.1016/j.proenv.2015.07.246.

Christopher, M., Paccapelo, V., Kelly, A., Macdonald, B., Hickey, L., Richard, C., Verbyla, A., Chenu, K., Borrell, A., Amin, A., Christopher, J., 2021. QTL identified for stay-green in a multi-reference nested association mapping population of wheat exhibit context dependent expression and parent-specific alleles. Field Crop. Res. 270, 108181 https://doi.org/10.1016/j.fcr.2021.108181.

Collins, B., Chapman, S., Hammer, G., Chenu, K., 2021. Limiting transpiration rate in high evaporative demand conditions to improve Australian wheat productivity. In silico Plants. https://doi.org/10.1093/insilicoplants/diab006.

Collins, B., Chenu, K., 2021. Improving productivity of Australian wheat by adapting sowing date and genotype phenology to future climate. Clim. Risk Manag. https://doi.org/10.1016/j.crm.2021.100300.

Djanaguiraman, M., Vara Prasad, P.V., Murugan, M., Perumal, R., Reddy, U.K., 2014. Physiological differences among sorghum (Sorghum bicolor L. Moench) genotypes under high temperature stress. Environ. Exp. Bot. 100, 43–54. https://doi.org/10.1016/j.envexpbot.2013.11.013.

Fernie, E., Tan, D.K., Liu, S.Y., Ullah, N., Khoddami, A., 2022. Post-anthesis heat influences grain yield, physical and nutritional quality in wheat: a review. Agriculture 12 (6), 886.

Field, C.B., Barros, V., Stocker, T.F., Dahe, Q., Jon Dokken, D., Ebi, K.L., Mastrandrea, M. D., Mach, K.J., Plattner, G.K., Allen, S.K., Tignor, M., Midgley, P.M., 2012. Managing the risks of extreme events and disasters to advance climate change adaptation: Special report of the intergovernmental panel on climate change. Managing the Risks of Extreme Events and Disasters to Advance Climate Change Adaptation: Special Report of the Intergovernmental Panel on Climate Change. doi: 10.1017/CBO9781139177245.

Frederiks, T.M., Christopher, J.T., Harvey, G.L., Sutherland, M.W., Borrell, A.K., 2012. Current and emerging screening methods to identify post-head-emergence frost adaptation in wheat and barley. J. Exp. Bot. 63, 5405–5416. https://doi.org/10.1093/jxb/ers215.

Gebeyehou, G., Knott, D.R., Baker, R.J., 1982. Relationships among durations of vegetative and grain filling phases, yield components, and grain yield in Durum wheat cultivars 1. Crop Sci. 22, 287–290. https://doi.org/10.2135/cropsci1982.0011183×002200020021x.

Gerard, G.S., Crespo-Herrera, L.A., Crossa, J., Mondal, S., Velu, G., Juliana, P., Huerta-Espino, J., Vargas, M., Rhandawa, M.S., Bhavani, S., Braun, H., Singh, R.P., 2020. Grain yield genetic gains and changes in physiological related traits for CIMMYT's high rainfall wheat screening nursery tested across international environments. Field Crop. Res. 249, 107742 https://doi.org/10.1016/j.fcr.2020.107742.

Girousse, C., Inchboard, L., Deswarte, J.-C., Chenu, K., 2021. How does post-flowering heat impact grain growth and its determining processes in wheat? J. Exp. Bot. https://doi.org/10.1093/jxb/erab282.

Guo, Z., Slafer, G.A., Schnurbusch, T., 2016. Genotypic variation in spike fertility traits and ovary size as determinants of floret and grain survival rate in wheat. J. Exp. Bot. 67, 4221–4230. https://doi.org/10.1093/jxb/erw200.

Jamieson, P.D., Brooking, I.R., Porter, J.R., Wilson, D.R., 1995. Prediction of leaf appearance in wheat: a question of temperature. Field Crop. Res. 41, 35–44. https://doi.org/10.1016/0378-4290(94)00102-I.

Limpens, J., Granath, G., Aerts, R., Heijmans, M.M.P.D., Sheppard, L.J., Bragazza, L., Williams, B.L., Rydin, H., Bubier, J., Moore, T., Rochefort, L., Mitchell, E.A.D., Buttler, A., van den Berg, L.J.L., Gunnarsson, U., Francez, A.J., Gerdol, R., Thormann, M., Grosvernier, P., Wiedermann, M.M., Nilsson, M.B., Hoosbeek, M.R., Bayley, S., Nordbakken, J.F., Paulissen, M.P.C.P., Hotes, S., Breeuwer, A., Ilomets, M., Tomassen, H.B.M., Leith, I., Xu, B., 2012. Glasshouse vs field experiments: Do they yield ecologically similar results for assessing N impacts on peat mosses? New Phytol. 195, 408–418. https://doi.org/10.1111/j.1469–8137.2012.04157.x.

Lobell, D.B., Hammer, G.L., Chenu, K., Zheng, B., McLean, G., Chapman, S.C., 2015. The shifting influence of drought and heat stress for crops in northeast Australia. Glob. Chang. Biol. 21, 4115–4127. https://doi.org/10.1111/gcb.13022.

Najeeb, U., Tan, D.K.Y., Sarwar, M., Ali, S., 2019. Adaptation of crops to warmer climates: morphological and physiological mechanisms. In: Sustainable Solutions for Food Security: Combating Climate Change by Adaptation. ⟨https://doi.org/10.1007/978–3-319–77878-5_2⟩.

Niinemets, Ü., Keenan, T.F., 2012. Measures of light in studies on light-driven plant plasticity in artificial environments. Front. Plant Sci. 3, 156. https://doi.org/10.3389/fpls.2012.00156.

Paleg, L.G., Aspinall, D., 1964. Effects of daylength and light intensity on growth of barley II. Influence of incandescent light on apical development. Bot. Gaz. 125 (3), 149–155.

Passioura, J.B., 2006. The perils of pot experiments. Funct. Plant Biol. 33, 1075–1079.

Poorter, H., Fiorani, F., Pieruschka, R., Wojciechowski, T., van der Putten, W.H., Kleyer, M., Schurr, U., Postma, J., 2016. Pampered inside, pestered outside? Differences and similarities between plants growing in controlled conditions and in the field. New Phytol. 212, 838–855. https://doi.org/10.1111/nph.14243.

Porter, J.R., Gawith, M., 1999. Temperatures and the growth and development of wheat: a review. Eur. J. Agron. 10, 23–36. https://doi.org/10.1016/S1161-0301(98)00047-1.

Prasad, P.V.V., Djanaguiraman, M., 2014. Response of floret fertility and individual grain weight of wheat to high temperature stress: sensitive stages and thresholds for temperature and duration. Funct. Plant Biol. 41, 1261–1269. https://doi.org/10.1071/FP14061.

Ray, D.K., Gerber, J.S., Macdonald, G.K., West, P.C., 2015. Climate variation explains a third of global crop yield variability. Nat. Commun. 6, 1–9. https://doi.org/10.1038/ncomms6989.

Rebetzke, G.J., Van Herwaarden, A.F., Jenkins, C., Weiss, M., Lewis, D., Ruuska, S., Tabe, L., Fettell, N.A., Richards, R.A., 2008. Quantitative trait loci for water-soluble carbohydrates and associations with agronomic traits in wheat. Aust. J. Agric. Res. 59, 891–905. https://doi.org/10.1071/AR08067.

Richard, C., 2017. Breeding Wheat for Drought Adaptation: Development of Selection Tools for Root Architectural Traits. ⟨https://doi.org/10.14264/uql.2017.1055⟩.

Saini, H., Aspinall, D., 1982. Sterility in wheat (*Triticum aestivum* L.) induced by water deficit or high temperature: possible mediation by abscisic acid. Funct. Plant Biol. 9, 529–537. https://doi.org/10.1071/pp9820529.

Sofield, I., Evans, L., Cook, M., Wardlaw, I., 1977. Factors influencing the rate and duration of grain filling in wheat. Funct. Plant Biol. https://doi.org/10.1071/pp9770785.

Stone, P.J., Nicolas, M.E., 1995. Effect of timing of heat stress during grain filling on two wheat varieties differing in heat tolerance. I. Grain growth. Aust. J. Plant Physiol. 22, 927–934. https://doi.org/10.1071/PP9950927.

Stone, P.J., Nicolas, M.E., 1998. The effect of duration of heat stress during grain filling on two wheat varieties differing in heat tolerance: grain growth and fractional protein accumulation. Aust. J. Plant Physiol. https://doi.org/10.1071/PP96114.

Streck, N.A., 2005. Climate change and agroecosystems: the effect of elevated atmospheric $CO_2$ and temperature on crop growth, development, and yield. Ciência Rural. https://doi.org/10.1590/s0103-84782005000300041.

Tashiro, T., Wardlaw, I., 1990. The response to high temperature shock and humidity changes prior to and during the early stages of grain development in wheat. Funct. Plant Biol. https://doi.org/10.1071/pp9900551.

R Core Team, 2018. R Development Core Team. R: a Language and Environment for Statistical Computing. R Foundation for Statistical Computing, Vienna, Austria, 2014. Google Sch.

Telfer, P., Edwards, J., Bennett, D., Ganesalingam, D., Able, J., Kuchel, H., 2018. A field and controlled environment evaluation of wheat (Triticum aestivum) adaptation to heat stress. F. Crop. Res. https://doi.org/10.1016/j.fcr.2018.09.013.

Telfer, P., Edwards, J., Norman, A., Bennett, D., Smith, A., Able, J.A., Kuchel, H., 2021. Genetic analysis of wheat (Triticum aestivum) adaptation to heat stress. Theor. Appl. Genet. https://doi.org/10.1007/s00122-021-03778-2.

Thistlethwaite, R.J., Tan, D.K.Y., Buckley, T.N., Trethowan, R.M., 2015. Identification of genetic variation in heat stress and mechanisms of tolerance in wheat. Procedia Environ. Sci. 29, 30. https://doi.org/10.1016/j.proenv.2015.07.139.

Thistlethwaite, R.J., Tan, D.K.Y., Bokshi, A.I., Ullah, S., Trethowan, R.M., 2020. A phenotyping strategy for evaluating the high-temperature tolerance of wheat. Field Crop. Res. https://doi.org/10.1016/j.fcr.2020.107905.

Ullah, N., Ababaei, B., Chenu, K., 2020. Increasing Heat Tolerance in Wheat to Counteract Recent and Projected Increases in Heat Stress † 3390. ⟨https://doi.org/10.3390/proceedings2019036132⟩.

Wheeler, T.R., Batts, G.R., Ellis, R.H., Hadley, P., Morison, J.I.L., 1996. Growth and yield of winter wheat (Triticum aestivum) crops in response to $CO_2$ and temperature. J. Agric. Sci. https://doi.org/10.1017/s0021859600077352.

Zadoks, J.C., Chang, T.T., Konzak, C.F., 1974. A decimal code for the growth stages of cereals. Weed Res. https://doi.org/10.1111/j.1365-3180.1974.tb01084.x.

Zheng, B., Chenu, K., Chapman, S.C., 2016. Velocity of temperature and flowering time in wheat - assisting breeders to keep pace with climate change. Glob. Chang. Biol. https://doi.org/10.1111/gcb.13118.

Zheng, B., Chenu, K., Fernanda Dreccer, M., Chapman, S.C., 2012. Breeding for the future: what are the potential impacts of future frost and heat events on sowing and flowering time requirements for Australian bread wheat (Triticum aestivum) varieties? Glob. Chang. Biol. https://doi.org/10.1111/j.1365-2486.2012.02724.x.